Available online at www.sciencedirect.com

ScienceDirect

Journal of Power Sources 181 (2008) 251–258

JOURNAL OF POWER SOURCES

www.elsevier.com/locate/jpowsour

The effect of low humidity on the uniformity and stability of segmented PEM fuel cells

Fang-Bor Weng, Bo-Shian Jou *, Chun-Wei Li, Ay Su, Shih-Hung Chan

Fuel Cells Research Center, Yuan Ze University, 135 Yuan-Tung Road, Chung-Li, Tao Yuan 320, Taiwan, ROC

Received 31 October 2007; received in revised form 14 December 2007; accepted 15 December 2007
Available online 3 January 2008

Abstract

The performance and stability of a PEMFC depends on many operating parameters. The measurement of local currents in PEMFC cells is an important tool for diagnoses and development of fuel cells. In this study, a segmented cell was developed, which could serve as an essential instrument to investigate the different operating conditions in the cells and stacks of technical relevance. In addition, the effects of different feed gas humidity and temperatures were investigated to analyze the steady-state performance, uniformity, and the local stability of PEMFC with the use of eight segmented regions. With this research method, the resistance in each segment could be measured by ac impedance as well as make a comparison between Nafion® 117 and 112 membranes in PEMFC. In the experiment, by probing into the high frequency internal resistance and performance of this cell, the effects of flow rates of fuels, oxidants, relative humidity, and directional channel flows were investigated for performance and stability of local segmented regions. The results of the experiments demonstrate that the local current distribution is strongly influenced by the relative humidity of fuel, the stoichiometric of the processed air, and the mode of operation. The cell was operated at a cell temperature of 50 °C with low relative humidity of 33% and 0%, causing the drying of the membrane (and increase of its resistance) at the top-stream path. The membrane conductivity was enhanced due to the water product increase by the reaction in the middle- and down-stream paths, because the down-stream has higher current than the top-stream. The relative humidity of the air increased along the path due to the product water, therefore, the current density increased as well. The local segmented cell could maintain stable performance at low hydrogen stoichiometry of 1.05 for low humidity gases. As the counter-flow and inverse gravity direction of hydrogen fuel was operated, the fuel cell showed the much more stable and uniform local performance.

Keywords: Segmented PEMFC; Current distribution; Relative humidity; Impedance measurement

1. Introduction

Polymer electrolyte membrane (PEM) fuel cells have been experimentally investigated for many years, especially on the topic concerning the relationship between various operating conditions and performance. The performance tests of the fuel cells in past studies could only demonstrate whole power, of current and voltage, for instance, when the fuel cells were operated in special conditions, such as flooded or dry, the whole performance had to be included in the results, there was no performance results of just the local areas. Generally, the commercial applications of PEMFCs are operated in the condition of low gas humidity in order to reduce an additional power loss, which is used for heat gas humidity. As we know, low gas humidity is the result in the decrease of water content in the PEMFC, which will cause the performance decline. In order to explore the phenomenon in dry operating conditions, it is important to measure the local currents in PEMFCs for future diagnoses and development.

Few literatures have investigated current distribution in PEMFC, except for the following. First, Rajalakshmi et al. [1] divided 370 cm^2 active electrode areas into 12 segments. As the humidification of the reactant gases increased, there was a slight decrease in the performance of the down-stream segments, which could be due to the excessive humidification or collection of water production from the top- and mid-stream segments. Namely, the increase in humidification temperature resulted in

* Corresponding author. Tel.: +886 3 4638800; fax: +886 3 4555574.
E-mail addresses: fangbor@saturn.yzu.edu.tw (F.-B. Weng), s937201@mail.yzu.edu.tw (B.-S. Jou).

0378-7753/$ – see front matter © 2008 Elsevier B.V. All rights reserved.
doi:10.1016/j.jpowsour.2007.12.078

the flooding of the electrode inside the cell, which led to poor performance at the down-stream segments. Additionally, Ghosh et al. [2] used 244 cm^2 active areas, divided into 20 equal segments, to measure the current density distribution. They observed that with the increase in the stoichiometry, the performance in each segment was more homogenous. In addition, with the increase of pressure in the inlet, the performance of the segments near the inlets became better. Natarajan and Nguyen [3] investigated local current densities of six segments along single gas channels. When the water removal rate was not sufficient, electrode flooding occurred in segments that were farthest from of the gas inlet. The increase of anode humid temperature resulted in the reduction of water removal rates from the cathode, by back diffusion, leading to performance reduction of down-stream segments. Then, Büchi et al. [4] developed four corner segments in the plate to measure the local currents. They reported that for the low air stoichiometric the current densities of the segments closer to the exit were lower than the current densities at the segments near the inlet. This was due to the higher relative decrease in oxygen concentration at the lower stoichiometric. If the cell was operated with air at dew point, much lower than the cell temperature, then the air-inlet produces the lowest current density because of the membrane drying. Dong et al. [5] described the results of a newly developed real-time technique for in situ measurement of water vapor distributions within the reactant flow channels of an operating PEMFC using a gas analyzer. The cell in their study was operated under; anode 100% and cathode 50% of the gas inlet humid temperature. Due to electro-osmotic drag and water diffusion from the anode to the dry cathode, cathode water fractions increased along the flow path.

The main reason of this present work was to establish a method for the measurement of current distribution in PEMFCs with large-area electrodes and to understand the flow distribution and water management under different operating conditions of the cell. This diagnostic tool can be useful when the stacks are being developed. The flow-field design can be optimized based on the segmented performance. This study provides a new method for measuring the current distribution using an ac impedance to diagnose the water distribution and its effects on the segments performance.

2. Experimental

2.1. Basic design of eight-segment fuel cell

Self-developed, eight-segmented fuel cells were designed and fabricated for the following experiments; the specifications of fuel cell are shown in Table 1. A schematic representation of the fuel cell arrangement is shown in Fig. 1(a) and (b). The eight-segment fuel cell assembly consists of polycarbonate plates, current collector plates, graphite plates, gasket layer, and the MEA, all of which were clamped, between two enclosure plates, held by eight M8 screw joints, each with a torque of approximately 30 kgf cm. There were eight big holes on the enclosure plates, big enough to avoid contact with current collector. The 15-mm thick polycarbonate plate had 8 troughs of 10-mm depth, at both anode and cathode sides, in order to contain 8 current collector plates and graphite plates. Polycarbonate plates served the function of preventing heat loss and of keeping the insulation between the segments. The current collector plates had the capability of conducting the electric current from the graphite plates, and the material is gold-coated brass. There were two kinds of shapes in current collectors; however, the shapes were in one piece. One is the rectangular with dimensions of 37 mm × 22 mm × 5 mm (length × width × depth), and the other is the cylinder with dimensions of φ10 mm × 30 mm (diameter × length). The electric wire of load was connected to the top facet of cylinder. The cylinder will also connect to "heat conduction plates", which is used to conduct the heat into the inside of the fuel cell from the heating plates. And it has a heating plate at anode and cathode side. In order to measure the current in each of eight segments, the graphite plates in both anode and cathode are divided into eight segments, which can be in the troughs of polycarbonate plates. In order to minimize the leakage between eight segment, the dimension of graphite plates and the troughs in polycarbonate were accurately, and each segment were apart. The flow fields in segments were designed to connect closely and exactly with those in the polycarbonate plates, as shown in Fig. 2. The design of the flow fields was serpentine with 6 channels; each channel was 1.5 mm in width, 3 mm in depth, and the ribs were 1.5 mm in width. On the anode and cathode side, there was the O-ring between the enclosure plate and polycarbonate plate to prevent gas leakage. In addition, every cylinder wore an O-ring at the bottom of the cylinder in order to prevent gas leakage. Electrodes were obtained from E-Tek 250-W; the diffusion layer was 0.35 mm in thickness. The dimension of each electrode piece was 20 mm × 35 mm (active area of 7 cm^2), and each electrode piece was cut from the procured electrode stock. The eight-segmented electrodes were hot pressed on Nafion® 117 and 112 membranes (145 mm × 145 mm) at 135 °C, and 50 psi for 30 s, and then 100 psi for 60 s.

The eight-segment fuel cell can measure each individual current, at each segment, under this particular design. The current corrector plate in each segment did not contact with one another, nor did they have conductance with the end plates. Therefore, each segment could be connected with its individual electronic load and measured under various operational conditions with no reciprocal influence.

Table 1
Specification of eight-segment fuel cell

Item	Illustration
Flow-field area	92 cm^2
Flow-field type	6 serpentines
Flow-channel depth	3 mm
Flow-channel width	1.5 mm
Flow-rib width	1.5 mm
Membrane manufacturer/type	DuPont/Nafion® 117 and 112
Electrode-layer manufacturer/type	E-Tek/250-W
Segment area	7 cm^2
Total segment area	56 cm^2
Fuel	Anode: H_2
	Cathode: air, O_2

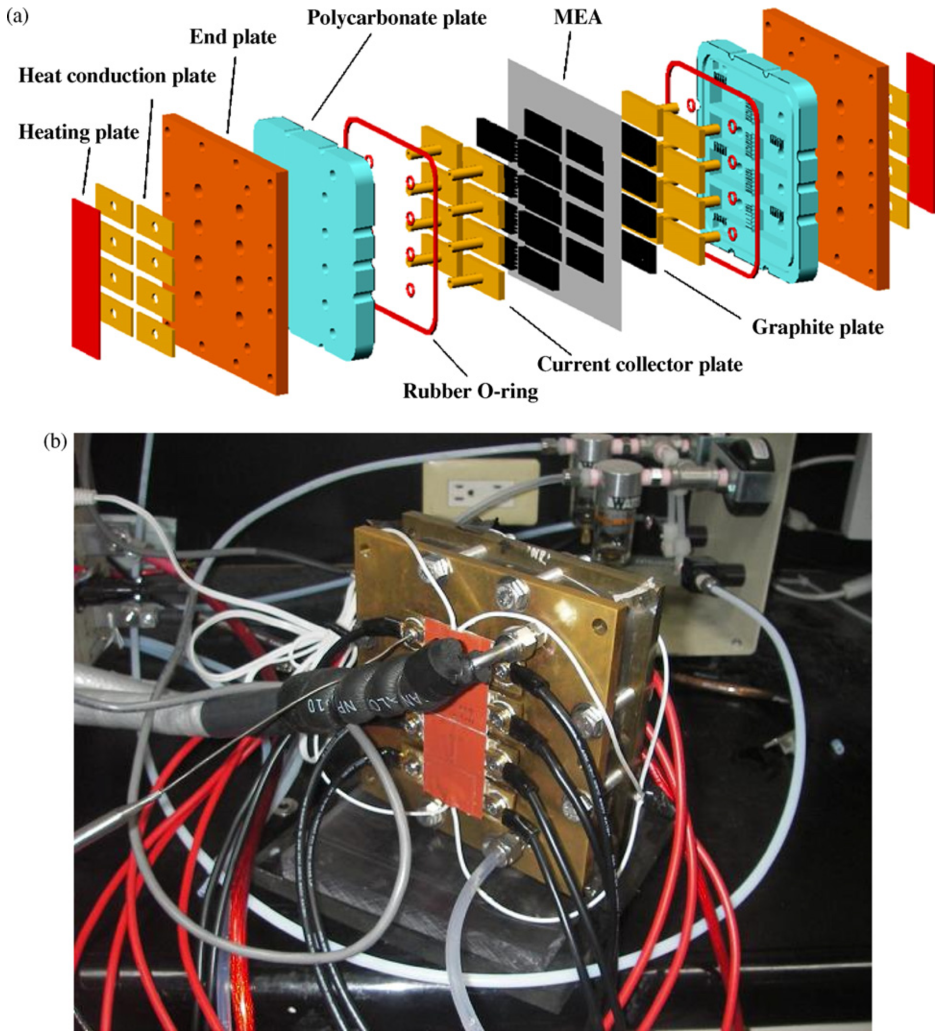

Fig. 1. (a) Schematic of the fabricated eight segments of fuel cells and (b) picture of eight segments of fuel cells under operation.

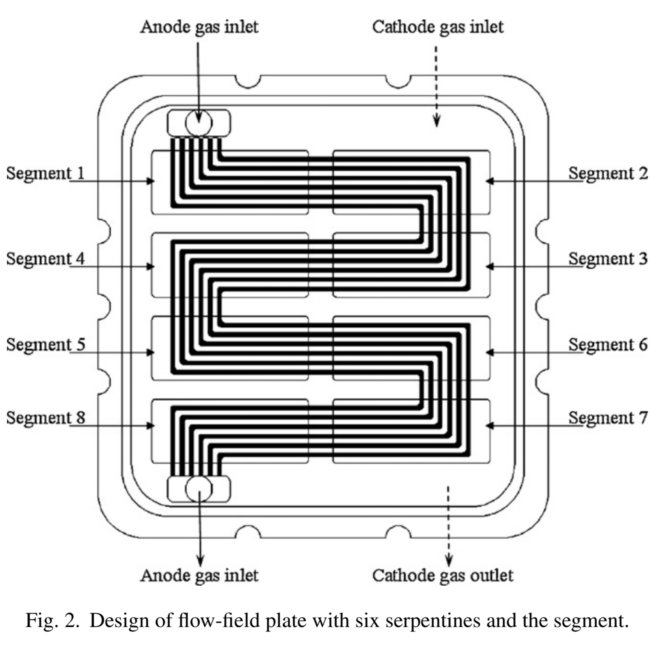

Fig. 2. Design of flow-field plate with six serpentines and the segment.

2.2. Measure procedures

In order to measure each segment's voltage and current, the current lines of every segment, in both anode and cathode, were connected to an electronic load box PRODIGIT 3311 D. In other words, there were eight load boxes to test the various series of experiments and simultaneously record individual data from each of the eight segments. Scribner 850 C fuel cell test loads were available and used for the impedance experiments. The set conditions of the impedance experiments in this study were at 0.5 V cell voltages, within a frequency range from 0.1 Hz to 10 kHz, and 10% of amplitude. Before testing the performance of the eight-segment fuel cell, MEA conditioning was performed with 0.6 V for 1800 s, then 0.4 V for 1800 s, and then with open circuit voltage for 60 s, which constitutes three stages. Repeating the three stages five to six times, or more, until the performance of each segment reached a relatively steady state [6]. The gas was humidified in a bubbler, and then mixed with dry gas to set the desired dew point temperature. Eight loads of PRODIGIT 3311 D were used for the various series of experiments, such as

Table 2
Baseline operating conditions

Parameter	Illustration
Anode gas/stoichiometric	H_2/1.05 or 2
Cathode gas/stoichiometric	Air/2
Operating pressure	1 atm
Cell temperature	50 °C
Anode inlet humidity	100% at 50 °C 50% at 30 °C 0% at gas bypass
Cathode inlet humidity	100% at 50 °C 50% at 30 °C 0% at gas bypass

scan voltage, constant voltage, and constant current. This study investigated two different membrane thicknesses of Nafion® 117 and 112 to observe the differences of the performances between the two kinds of membrane thicknesses at low gas humidity for different operating conditions, as shown in Table 2.

3. Result and discussion

3.1. The effects of low humidity on Nafion® 117

The current responses of the eight segments in Nafion® 117 are shown in Fig. 3, with the help of polarization curves. These curves show that the segment performances under the chosen experimental conditions were reasonably uniform. Segment 8 consistently performed the best, whereas segment 6 showed the poorest performance. With this fuel cell hardware, the difference of performance was caused by operating conditions, such as the gas flow rate, gas humid temperature, cell temperature, oxygen, air, back pressure, etc. In order to reduce the factors of operating conditions, which resulted in the unevenness of performance among the eight segments, the fuel cell was operated with sufficient fuel flow and gas humidity conditions. In the experimental conditions of Fig. 3, the performance difference in the segments may be attributed to inherent variations in the

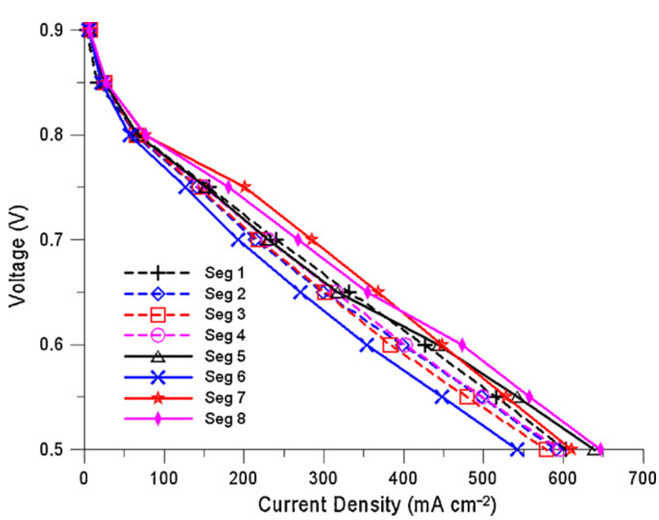

Fig. 3. Polarization curves of eight segments, Nafion 117, H_2/O_2 constant flow: 500 $cm^3\ min^{-1}$, cell temperature 50 °C, humidified gas temperature 55 °C.

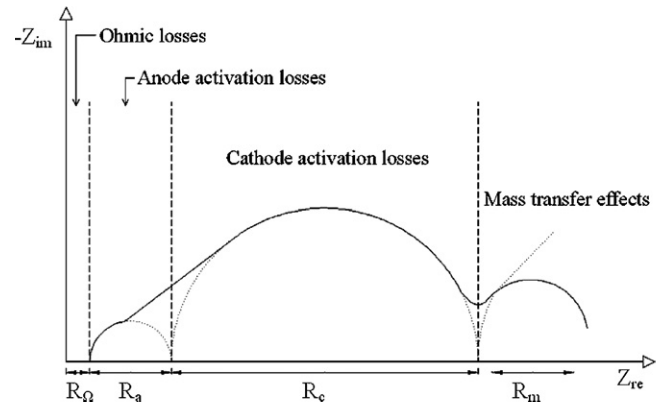

Fig. 4. Nyquist plot from hypothetical fuel cells. The four regions represent four losses in the fuel cells, and the size of each loop is correlated to the relative magnitude of each loss.

GDL and catalyst layer properties. In addition, Nafion® 117, under fully humid operations, may result in uneven flooding, as was discussed later.

The Nyquist plot is one of the popular formats for evaluating electrochemical impedance data, a schematic drawing of a Nyquist plot is shown in Fig. 4, according to both the published works [7,8] and the experimental results. This schematic description allows better understanding of the in situ impedance data on the Nyquist plots. In Fig. 4, the resistance R_Ω represents the total ohmic resistance of the fuel cell. Resistance of a single cell component consisted of the ohmic resistance of the membrane R_m, anode R_a, and cathode R_c. The total ohmic resistance changes with the humidity of the membrane at room temperature [9].

Fig. 5(a) shows 100% of gas humidity at both anode and cathode at the condition of a constant voltage of 0.5 V for 60 min in the eight segments; the other operating condition refers to case 1 of Table 3. In this figure, top and middle stream of the path (from one to six) had constant increases of current, and downstream path (seven and eight) had gradually decreased in current. Although the down stream of the path had a higher current than the top and middle streams, at the end of the first 30-min period, the current decayed significantly after the first 30 min, the current of the down stream was lower than that of the top and middle streams. In order to analyze the phenomenon of current increase to the top and middle streams, with a decrease of current in the down stream, there were four impedance measure points in the constant voltage curve. Z1 represents the current curve at the 10 min mark of the experiment; Z2 refers to the current curve at the 50 min mark, both of which were measured in segment 1; Z3 shows the current curve at the 10 min mark; and Z4 at the 50 min mark, both of which were measured in segment 8, all of which are shown in the Nyquist plot of Fig. 5(b). This figure demonstrates that, with time Z2 had a smaller size of semicircle than Z1. In addition, the semicircle of Z2 was slightly to the left of Z1, meaning that top and middle streams in the fuel cell had more humidity and greater anode, and cathode activation, which caused higher currents in top and middle streams. The reason for the gradual increase of current in top and middle streams might be, the top and middle streams of the cell had

Table 3
Operating condition of Nafion 117 in four cases

	Stoichiometries of gas, H_2/air	Cell temperature (°C)	Relative humidity (%)	Load mode	Flow direction
Case 1 (Fig. 5)	1.2/2.0	50	100	Constant voltage at 0.5 V	Fuel inlet in segment 1
Case 2 (Fig. 6)	1.2/2.0	50	33	Constant voltage at 0.5 V	Fuel inlet in segment 1
Case 3 (Fig. 7)	1.2/2.0	50	50	Constant voltage at 0.5 V	Fuel inlet in segment 8 (counter-flow)
Case 4 (Fig. 8)	1.2/2.0	50	50	Constant current at 1 A	Counter-flow

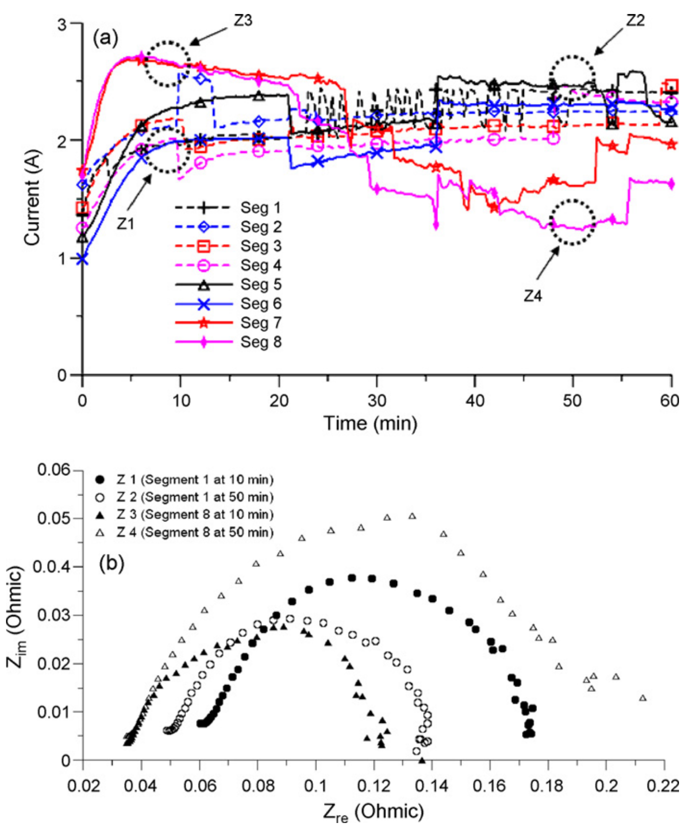

Fig. 5. Case 1: (a) relative humidity: 100% and (b) Nyquist plot.

a shortage of water at the beginning of the experiment. When the current was stable with the increase of water required by the membrane, then those segment cells in the top and middle streams produced more water and generated higher currents. Z4 had a bigger semicircle than Z3, which was attributed to the phenomenon that the down stream obtains more and more water from the top and middle streams. Therefore, the water accumulated in the down stream blocks the proton conduct area, at anode and cathode, which resulted in the increase of catalyst resistance. However, the membrane resistance of Z4 was similar to that of Z3, meaning that the water content of the membrane in the down stream had not changed. The cell was operated at 33% of gas humidity at anode and cathode; the results are shown in Fig. 6(a). In this figure, the current in the top stream was probably less because of the condition of low gas humidity, which resulted in membrane dryness for the fuel cell. The down stream had more water and it had a higher current than that of the top and middle streams. The above statements can be explained with ac impedance, as is shown in Fig. 6(b).

In order to examine the effects of counter-flow gas from fuel cells, the inlet and outlet were exchanged in the anode side, i.e. the inlet of segment 1 in the anode was changed to the inlet of segment 8. A constant voltage of 0.5 V for 60 min at all eight segments, as is shown in Fig. 7(a). Because the fuel cell is operated under the condition of low humidity, the current of each segment slightly decreased with time. Segment 7 possessed the best performance. It is noteworthy that the current in segment 5 was similar to segment 8, which resulted from the condition that, the inlet in the fuel cell was changed to the down stream in the flow path. Therefore, the water reserve from the cathode to the anode was brought from the middle and top streams. The sequence of the humidity of membrane from high to low is down, middle, and top streams. With the testing method of ac impedance are shown in Fig. 7(b). The eight-segment fuel cell operated under the condition of counter-flow with operating conditions of constant current 1 A for 60 min at all eight segments, as is shown in Fig. 8(a). From Fig. 8(a) it can be observed that the voltage in each segment was uniform; in addition, the voltage curve generally remained at 0.6 V. In Fig. 8(a), the four aspects

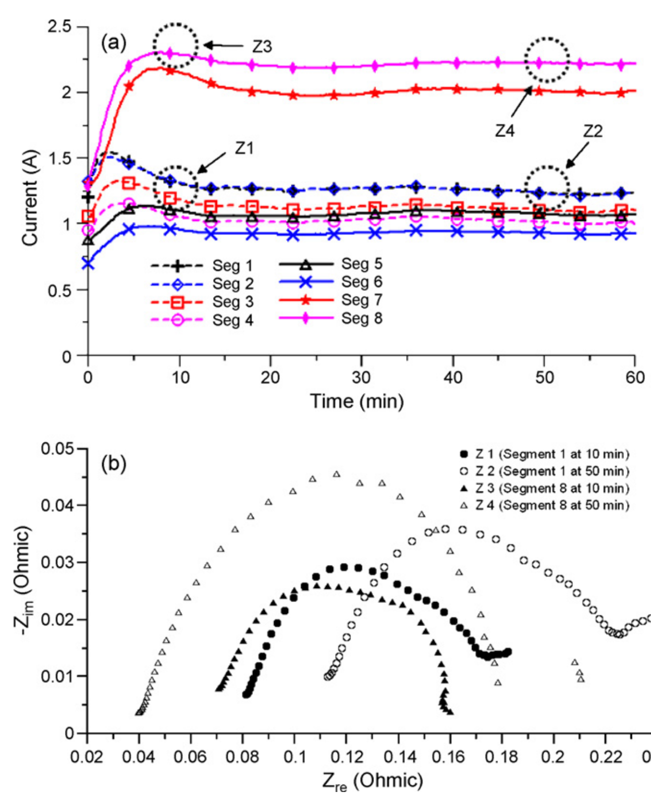

Fig. 6. Case 2: (a) relative humidity: 33% and (b) Nyquist plot.

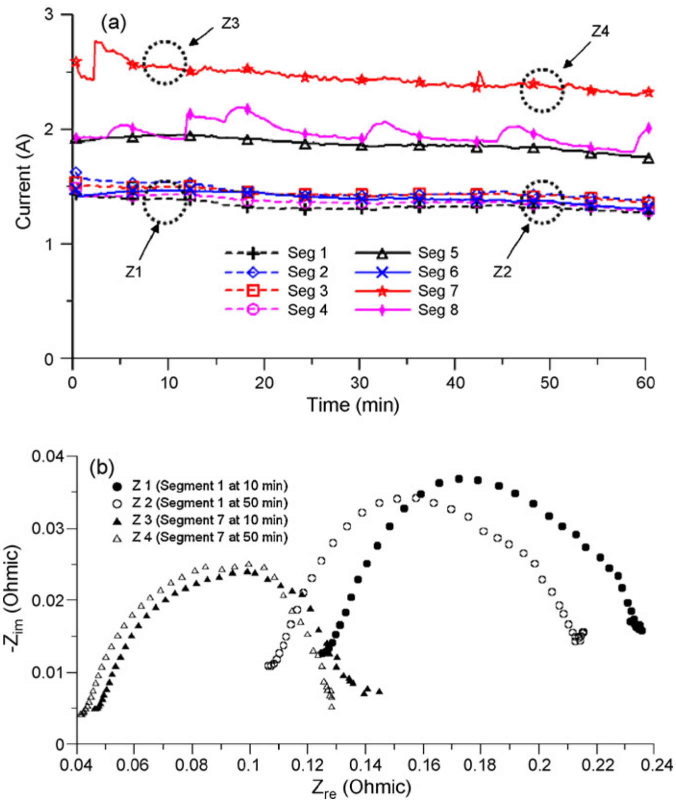

Fig. 7. Case 3: (a) stability of constant voltage at 0.5 V, gas counter-flow and (b) Nyquist plot.

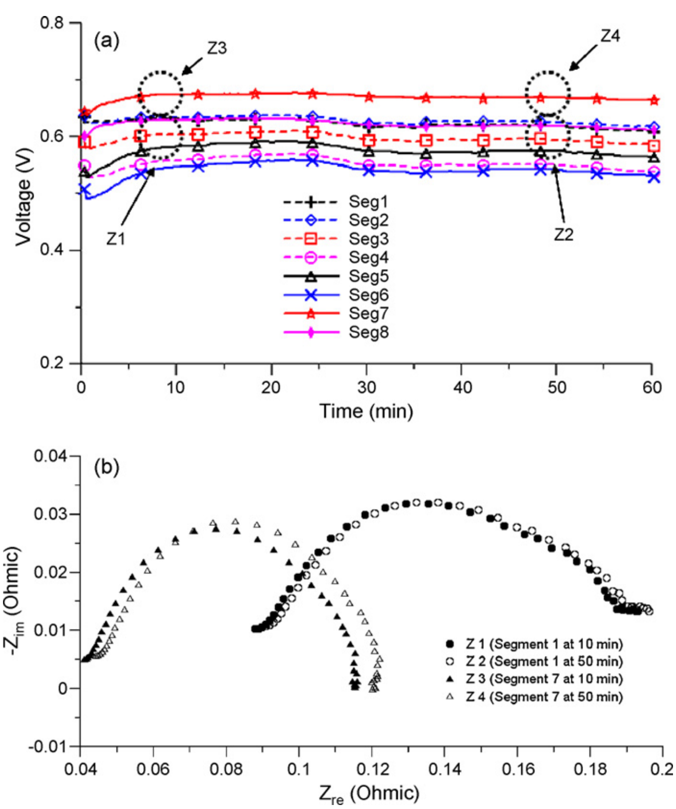

Fig. 8. Case 4: (a) stability of constant current at 1 A, gas counter-flow and (b) Nyquist plot.

measured with the use of ac impedance to observe resistance in the fuel cell are shown in Fig. 8(b). The Nyquist plot, with the use of ac impedance, can explain why the voltage in eight segments was stable and uniform under the operating condition of constant current. In addition, the water generated was the same as well, because the current was produced in each segment at a constant current. Moreover, the water steam in the down stream of the cathode could be carried by fuel to the middle and top streams, which were easy membrane drying, which resulted in higher membrane resistance at the top stream of the cathode.

The summary of membrane conditions and performance in segments are shown in Table 4. In this table, case 1 was the condition of fully gas humidity, but it was the only one with unstable curve in segments. Case 4 present the stable curve and uniform performance in segments. The result prevented the MEA in the fuel cell from segmental degradation, which, after a long-time operation increased the longevity of the MEA.

3.2. *The effect of low humidity on Nafion® 112*

In order to analyze the effects, on all eight segments, exerted by Nafion® 112, several experiments of various operational conditions were conducted, which demonstrated the measurement of high frequency cell resistance in the current interrupt method for the total cell. The meaning of resistance (R) is related to proton conductivity (σ), the lower resistance provides the better membrane conductivity. $I_{H^+} = (\sigma A)\Delta V_R/l_m$. Therefore, the high frequency cell resistance was $\Delta V_R/I_{H^+} = l_m/(\sigma A) = R$. Fig. 9 was drawn based on the operating condition of the cell temperature at 50 °C, with a constant voltage of 0.5 V for 60 min, 100% gas humidity in anode and cathode, and the stoichiometric were 1.2 and 2 in anode and cathode, respectively. Compared with Nafion® 117 under the same operating condition, the current of each segment in Nafion® 112 was stable and uniform, which was unlike Nafion® 117, in which the excessive water caused flooding in the down stream with the passing of time. Because Nafion® 112 had better proton conductivity, the current generated in each segment was greater; the greater current produced more gas flow; therefore, the stability of Nafion® 112 was much better than that of Nafion® 117.

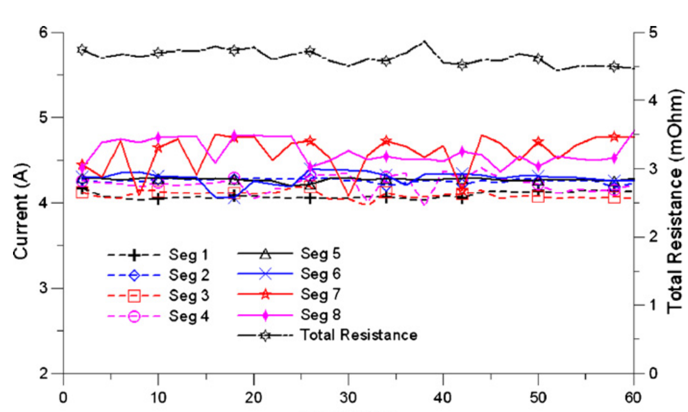

Fig. 9. Stability of constant voltage at 0.5 V, Nafion 112, H_2/air stoichiometric: 1.2/2.0, cell temperature 50 °C, relative humidity: 100%.

Table 4
Summary of membrane conditions in eight-segment fuel cell

	Case 1	Case 2	Case 3	Case 4
Top stream (10 min)	Dry	Dry	Dry	Saturate
Top stream (50 min)	Saturate	Dry	Saturate	Saturate
Down stream (10 min)	Saturate	Dry	Dry	Saturate
Down stream (50 min)	Saturate and flooding	Saturate	Saturate	Saturate
Performance in segments	Unstable curve, non-uniform	Stable curve, non-uniform	Stable curve, non-uniform	Stable curve, uniform

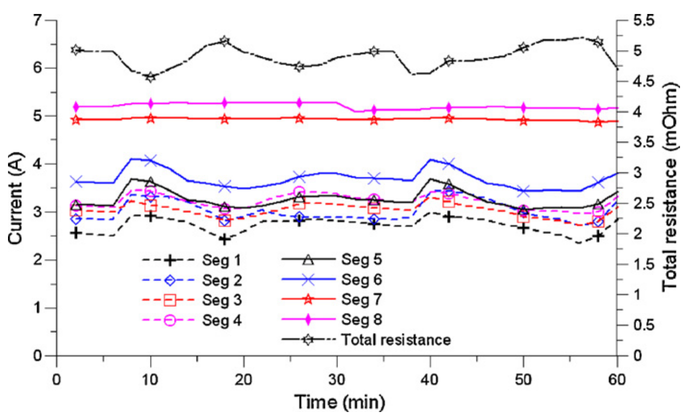

Fig. 10. Stability of constant voltage at 0.5 V, Nafion 112, H_2/air stoichiometric: 1.2/2.0, cell temperature 50 °C, relative humidity: 33%.

In Fig. 10, the gas humidity in anode and cathode decreased to 33%, under various operating conditions, similar to Fig. 9. There were two groups of current curves similar to Fig. 6(a); one group stands for the current in the top and middle streams, and the other one stands for the down stream. Moreover, the down stream had a higher current, similar to that in Fig. 6(a), because under the condition of low humidity, the top and middle streams brought water to the down stream, and then the down stream showed better performance. As for the adulatory phenomenon of current and total ohmic resistance in the top and middle streams, as shown in Fig. 10, the water product was washed away by gas, then caused immediate humidity and drying of the membrane.

When the gas humidity was decreased to 0%, there was no gas humidity at the anode and cathode, as is shown in Fig. 11. It is clear to see that the current in the top and middle stream was continuously decreasing; however, the current in the down stream was stable. This is because, in the condition of no gas humidity, the water in the top and middle streams was brought to the down stream, causing the membrane to dry in the top and middle streams, as the membrane remained wet in the down stream. As for the aspect of total cell resistance, resistance was seen to decline continuously, which could also explain why the current in the top and middle streams declined continuously.

If under the operating condition in Fig. 11, with the change of gas stoichiometric to 1.05 in the anode, it becomes the operating conditions from Fig. 12. Compared to Fig. 11, the current of all segments in Fig. 12 decreased, however, the current distribution in the top, middle, and down streams was more, uniform in Fig. 11. This is because when the gas flowed in the anode, it was not easy for the water to flow to the down stream. Therefore, the current in the top and middle streams did not decline continuously, leaving the current in the down stream as similar to that in the top and middle streams, because of the shortage of water. Accordingly, it can be concluded that, when the fuel cell was operated under the condition of low gas humidity and the least stoichiometric, the performance of each segment was more stable to prevent membrane drying, although the overall performance of the fuel cells was worse.

Under the conditions of membrane with Nafion® 112, counter-flow and inverse direction of the hydrogen fuel was also performed, which is shown in Fig. 13. The time-period of testing was twice as long as the pervious experiment. Although the overall performance slightly declined, and total cell resistance went up slightly as well, the current in each segment under counter-flow was more stable and uniform as compared to Fig. 12. This may be due to, fuel entering the down stream of the cathode

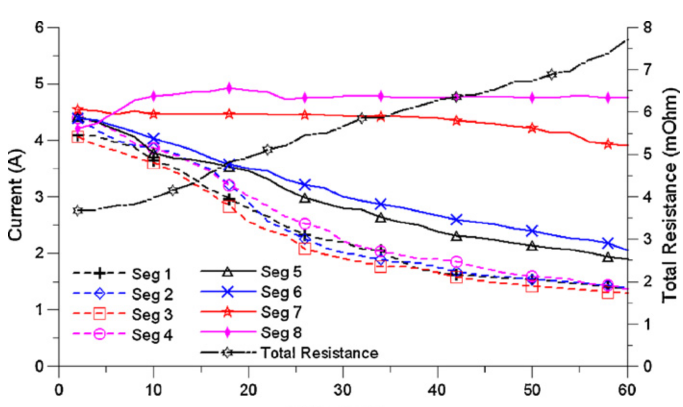

Fig. 11. Stability of constant voltage at 0.5 V, Nafion 112, H_2/air stoichiometric: 1.2/2.0, cell temperature 50 °C, relative humidity: 0%.

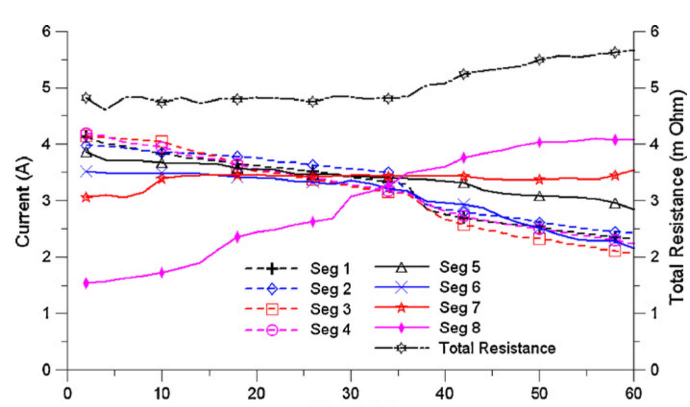

Fig. 12. Stability of constant voltage at 0.5 V, Nafion 112, H_2/air stoichiometric: 1.05/2.0, cell temperature 50 °C, relative humidity: 0%.

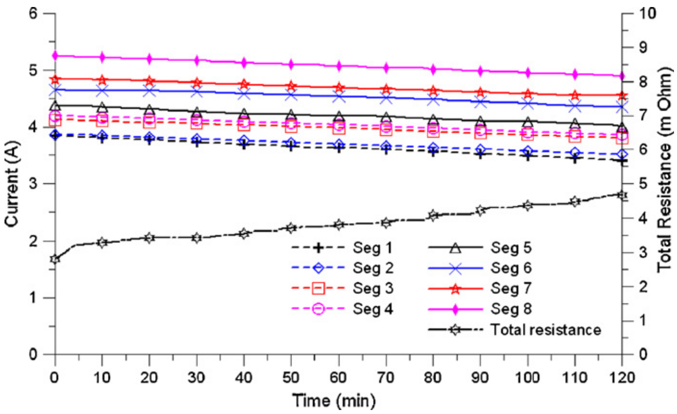

Fig. 13. Stability of constant voltage at 0.5 V, Nafion 112, H_2/air stoichiometric: 1.05/2.0, cell temperature 50 °C, relative humidity: 0%, gas counter-flow.

carrying part of the water to the middle and top streams of the cathode, thereby causing the humidity in each segment to be generally the same. Under this operating method, it was helpful to avoid unevenness of drying membrane and degradation in the fuel cells.

4. Conclusion

In this paper, the effects of different feed gas humidity and temperatures were investigated to analyze the performance uniformity of PEMFC, with the use of completely eight-segmented regions. With this method, the resistance in each segment could be measured by ac impedance, as well as making a comparison between Nafion® 117 and 112 membranes under low humid conditions. In the fuel cell using Nafion® 117, and with the operating condition of low humidity, there where uneven performances at top, middle, and down stream. When the gas inlet direction was altered into the counter-flow, the uneven performance was decreased in the eight segments of the fuel cell. When Nafion® 112 was used for the membrane in the fuel cell, there was better proton conductivity; this fuel cell could be operated under very low gas humidity, and gas stoichiometric, and produced better performance uniformity, as compared to the Nafion® 117. When a gas inlet direction was altered into the condition of the counter-flow, the current in all eight segments was stable and uniform, under Nafion® 112, with low anode stoichiometric of 1.05 and 0% of gas humidity. This was helpful for uniform performance in each segment; reducing the uneven degradation in the fuel cells.

Acknowledgments

We gratefully acknowledge the financial support of the Technology Development Program to Academia, DIT Department, the Ministry of Economic Affairs, Taiwan, and the ROC under grant No. 94-EC-17-A-05-S1-0012. In addition, the Aim for the International Top, University Program, the Ministry of Education, under grant No. 0950026846, and the Research Team Members in the Yuan Ze Fuel Cell Center.

References

[1] N. Rajalakshmi, M. Raja, K.S. Dhathathreyan, J. Power Sources 112 (2002) 331–336.
[2] P.C. Ghosh, T. W¨uster, H. Dohle, N. Kimiaie, J. Mergel, D. Stolten, J. Power Sources 154 (2006) 184–191.
[3] D. Natarajan, T.V. Nguyen, AICHE J 51 (2005) 2587–2598.
[4] F.N. Büchi, A.B. Geiger, R.P. Neto, J. Power Sources 145 (2005) 62–67.
[5] Q. Dong, J. Kull, M.M. Mench, J. Power Sources 139 (2005) 106–114.
[6] F.B. Weng, B.S. Jou, A. Su, S.H. Chan, P.H. Chi, J. Power Sources 171 (2007) 179–185.
[7] R. O'Hayre, S.W. Cha, W. Colella, F.B. Prinz, Fuel Cell Fundamentals, vol. 203, John Wiley and Sons, Inc., New Jersey, 2005, p. 212.
[8] M. Ciureanu, R. Roberge, J. Phys. Chem. B 105 (2001) 3531–3539.
[9] W.H. Zhu, R.U. Payne, B.J. Tatarchuk, J. Power Sources 168 (2007) 211–217.